

**Solar neutrino fluxes with arbitrary  $^3\text{He}$  mixing**V. Berezhinsky,<sup>1,\*</sup> G. Fiorentini,<sup>2,†</sup> and M. Lissia<sup>3,‡</sup><sup>1</sup> *Istituto Nazionale di Fisica Nucleare, Laboratori Nazionali del Gran Sasso,  
I-67010 Assergi (AQ), Italy*<sup>2</sup> *Dipartimento di Fisica dell'Università di Ferrara and  
Istituto Nazionale di Fisica Nucleare, Sezione di Ferrara, I-44100 Ferrara, Italy*<sup>3</sup> *Istituto Nazionale di Fisica Nucleare, Sezione di Cagliari and  
Dipartimento di Fisica dell'Università di Cagliari, I-09042 Monserrato (CA), Italy*  
(January 24, 1999; revised August 10, 1999)**Abstract**

The  $^3\text{He}$  abundance is not constrained by helioseismic data. Mixing of  $^3\text{He}$  inside the solar core by processes not included in the solar standard model (SSM) has been recently proposed as possible solution to the solar neutrino problem. We have performed a model independent analysis of solar neutrino fluxes using practically arbitrary  $^3\text{He}$  mixing. In addition, we have been simultaneously varying within very wide ranges the temperature in the neutrino production zone and the astrophysical factors,  $S_{17}$  and  $S_{34}$ , of the  $p + ^7\text{Be}$  and  $^3\text{He} + ^4\text{He}$  cross sections. Seismic data are used as constraints, but the solar-luminosity constraint is not imposed. It is demonstrated that even allowing  $^3\text{He}$  abundances higher by factors up to 16 than in the SSM, temperatures 5% (or more) lower, the astrophysical factor  $S_{17}$  up to 40% higher, and varying  $S_{34}$  in the range (-20%, +40%), the best fit is still more than  $5\sigma$  away from the observed fluxes. We conclude that practically arbitrary  $^3\text{He}$  mixing combined with independent variations of temperature and cross-sections cannot explain the observed solar neutrino fluxes.

**I. INTRODUCTION**

Detected neutrino fluxes in all five solar neutrino experiments (Homestake [1], SAGE [2], GALLEX [3], Kamiokande [4], and Superkamiokande [5]) are smaller than those predicted by SSM's. The status of the solar neutrino measurements is that of *disappearance oscillation experiments*.

How reliable is this conclusion? In other words, how reliable are the SSM predictions of solar neutrino fluxes?

1. *Helioseismic observations* of density and sound-speed-squared profiles are in agreement with SSM predictions throughout the sun with an accuracy better than a fraction

of percent [6]. This agreement was recently found to be valid also in the inner solar core,  $R \leq 0.1R_\odot$ , where neutrino fluxes are mostly produced [7–11].

In the literature the relevance of this agreement for the neutrino fluxes has been questioned with two kinds of objections.

First, seismic measurements give only the sound speed squared,  $c_s^2$ , but not directly the temperature  $T$ , which is mostly relevant for neutrino production. The connection between the uncertainties of  $c_s^2$  and  $T$  is  $\delta c_s^2/c_s^2 = \delta T/T - \delta\mu/\mu$ , where  $\mu$  and  $\delta\mu$  are the molecular weight and its uncertainty. In principle, one can imagine that  $\delta T/T$  much larger than  $\delta c_s^2/c_s^2$  could be compensated by correlated changes of the molecular weight. Note, however, that this compensation (fine tuning) should work for all distances, and this is harder to imagine.

Second, seismic uncertainties grow for  $R < 0.05R_\odot$ . Nevertheless, these uncertainties are too small to solve solar-neutrino problem. Careful analyses of the inversion method and of the available helioseismic data produce  $c_s^2$  in the agreement with the SSM value at level of 1% at  $R = 0$ , and better in the neutrino production zone [12].

2. *Nuclear cross-sections* for neutrino production could be responsible for the observed neutrino deficit.

Recent measurements [13] of the  ${}^3\text{He} + {}^3\text{He}$  cross section at the energy of the Gamow peak in the sun have eliminated a dangerous source of potential uncertainty. Moreover, even before this experiment, it had been already demonstrated that any combination of unknown cross sections and variations of central temperature cannot not explain the combined results of solar-neutrino experiments [14].

As everything in the world, SSM is not perfect. It does not include, for example, rotation and hydrodynamical processes. A bump in the sound-speed profile at  $R \approx 0.7R_\odot$  shows statistically significant disagreement between SSM and helioseismic observations. Nevertheless, this disagreement is far too small to affect neutrino fluxes. It is also most likely that rotation and hydrodynamical processes do not affect neutrino fluxes either. Indeed, in the region where statistically significant deviations from the SSM predictions are seen, helioseismology is a much more sensitive probe of the solar structure than neutrino experiments.

Lithium depletion is another problem for SSM's. The observed surface abundance of lithium in the sun (and other main sequence stars) is much lower than the one predicted by SSM's. This problem can be solved by anomalous diffusion, which drives lithium inside the sun, where it burns. This diffusion could be induced by gravity waves [15].

Gravity-wave induced diffusion is a mechanism of mixing inside the solar core. Another mixing mechanism, periodical instabilities, has been considered again and again in the literature starting with the pioneering work by Dilke and Gough [16]. Mixing in the solar core affects the solar neutrino fluxes, but it should be shown to be consistent with the other data; in general, large mixing contradicts seismic observations. Indeed, mixing episodes transport from the periphery to the center of the sun not only the desirable  ${}^3\text{He}$  or lithium but also large masses of hydrogen. The consequent reduction of the molecular weight increases the sound speed. This is the main problem of the Cummings-Haxton assumption [17] about mixing in the solar core: the resulting sound speed is too high [18]. Brun *et al.* [11] recently found that seismic data do not support even small mixing in the solar core. Using the turbulent diffusion coefficient suggested by Morel and Schatzman [19], they obtained a sound-speed profile in contradiction with observations.

The essence of the recent attempts to reconcile the observed neutrino fluxes with solar

models [20,17,15,21] consists in bringing  ${}^3\text{He}$  in the solar core by one mechanism or another. Arguments against these mechanisms use the *accompanying* processes, such as the simultaneous bringing-in of hydrogen. The strategy of our work is different: we allow arbitrary mixing of  ${}^3\text{He}$ , not accompanied by other elements. Moreover, we do not assume that the arriving  ${}^3\text{He}$  is in nuclear equilibrium with the other elements; an example can be the out-of-equilibrium concentration of  ${}^3\text{He}$  in mixing episodes caused by instability. Nonequilibrium burning of  ${}^3\text{He}$  lowers the temperature. We shall allow *independent* variation of temperature within  $\pm 5\%$  of its SSM value, assuming that some miraculous fine-tuning keeps the sound speed in agreement with seismic observations. In the solar core we also allow radial profiles of temperature and  ${}^3\text{He}$  density different from the SSM ones. In addition, we vary the two relevant cross-sections,  $S_{17}$  and  $S_{34}$ , within very generous ranges.

We shall demonstrate that the resulting predictions are, nonetheless, incompatible with the observed neutrino fluxes.

## II. ASSUMPTIONS, CONSTRAINTS AND NOTATION

We shall study the production of boron ( ${}^8\text{B}$ ) and beryllium ( ${}^7\text{Be}$ ) neutrinos. Our approach consists in comparing the calculated fluxes ( $\Phi_B, \Phi_{Be}$ ) with the observed ones.

Inspired by the SSM, we consider an effective Neutrino Production Zone (NPZ) for boron and beryllium neutrinos. In the SSM the production of B and Be neutrinos has its maximum at  $r = R_{NPZ} \approx 0.05R_\odot$ . When non-SSM profiles are considered, the position of this maximum changes. In our calculations we use  $R_{NPZ}$  only as a reference radius and take into account that the peak of the B-neutrino production does not coincide with that for Be-neutrinos. All quantities evaluated at  $r = R_{NPZ}$  are denoted by the index *NPZ*, *e.g.*,  $T_{NPZ}$  (temperature),  $\rho_{NPZ}$  (density),  $Y_{3,NPZ}$  ( ${}^3\text{He}$  abundance), etc. Temperature, density and abundance profiles will be specified.

We assume that  ${}^3\text{He}$  is transported to NPZ by some unspecified process and characterize it by the arbitrary value  $Y_{3,NPZ}$ . We do not assume local nuclear equilibrium for  ${}^3\text{He}$ : during mixing episodes, “fresh”  ${}^3\text{He}$  can be brought inside from the outer shells and burned in a nonequilibrium regime. However, it is easy to see that thermal equilibrium is established very fast and thus  ${}^3\text{He}$  has the thermal distribution of the surrounding gas.

We keep  $Y_{3,NPZ}$  and  $T_{NPZ}$  as independent parameters. In a realistic solar model increasing  $Y_{3,NPZ}$  increases the  ${}^3\text{He} + {}^3\text{He}$  reaction rate more than the rate of the  ${}^3\text{He} + {}^4\text{He}$  reaction, and the temperature must be lowered to keep the luminosity constant; the net result would be the decreasing of  $\Phi_{Be}$  and  $\Phi_B$ . In fact, in the SSM one finds that  $Y_3 \sim T^{-7}$ . For our purpose, any dependence between  $Y_{3,NPZ}$  and  $T_{NPZ}$  imposes additional restrictions and makes our conclusions stronger.

We do not impose the luminosity constraint. The luminosity sum rule is only used to express the *pp* neutrino contribution to the gallium experiments in terms of the other fluxes.

The CNO neutrino flux is conservatively neglected to avoid solar-model-dependent consideration. Including the CNO neutrino production would only strengthen our conclusions.

*Helioseismic constraints* are used very conservatively. We assume that temperature in the solar core can differ from that of the SSM by  $\pm 5\%$ , to be compared with a fraction of

percent allowed for the sound speed squared  $c_s^2$ . More specifically, we assume the following maximum range of temperature variation:

$$0.95 < T_{NPZ}/T_{NPZ}^{SSM} < 1.05, \quad (1)$$

and the same order of variation for the radial profile of the temperature in the NPZ.

The sound speed squared is given by  $c_s^2 = \gamma RT/\mu$ , where  $\gamma$  and  $R$  are constant,  $T$  is the temperature, and  $\mu$  the mean molecular weight,  $1/\mu = 2X + 3Y/4 + Z/2 \approx (5/4)(X + 3/5)$ . Therefore, since the accuracy of seismic determination of the sound speed is better than 1%, the following constraint must be met:

$$\frac{X(r) + 3/5}{X^{SSM}(r) + 3/5} = \frac{T^{SSM}(r)}{T(r)}. \quad (2)$$

Since the allowed variation of  $T(r)$  is only a few percent, one can use

$$X(r) = X^{SSM}(r) \quad (3)$$

with the accuracy needed: a few percent change in the temperature strongly affects neutrino production, while the same variation of  $X$  does not do much.

For the  ${}^4\text{He}$  abundance we use  $Y \approx 1 - X$ .

We can use the SSM density profile,  $\rho(r)$ , since this profile has been measured by seismic observations.

*The astrophysical factors* that affect B and Be neutrino production are  $S_{17}$  and  $S_{34}$ .

For the reaction  $p + {}^7\text{Be}$  the INT Collaboration [22] (1998) suggests the  $1\sigma$  range  $S_{17} = 19_{-2}^{+4}$  eV b; Castellani *et al.* [23] (1997) suggest  $S_{17} = 22.4 \pm 2.1$  eV b. The BBP98 SSM [10] and the BTCM SSM [11] use 19 eV b, while the DS96 SSM [24] uses 17 eV b. We shall use the generous range:

$$13 < S_{17} < 31 \text{ eV b.} \quad (4a)$$

For the reaction  ${}^3\text{He} + {}^4\text{He}$  the INT Collaboration [22] suggests the  $1\sigma$  range  $S_{34} = 0.53 \pm 0.05$  keV b; Castellani *et al.* [23] suggest  $S_{34} = 0.48 \pm 0.02$  keV b. The BBP98 SSM [10] and the BTCM SSM [11] use 0.53 keV b, while the DS96 SSM [24] uses 0.45 keV b. We consider the range:

$$0.38 < S_{34} < 0.68 \text{ keV b.} \quad (4b)$$

The *detected neutrino fluxes* used in our analysis are the following.

For the Chlorine signal we use the Homestake data  $2.56 \pm 0.21$  SNU [1]; for B-neutrino flux the Superkamiokande data  $\Phi_B = (2.46 \pm 0.09) \times 10^6 \text{ cm}^{-2}\text{s}^{-1}$  [5]; and for gallium signal we use the weighted average of the GALLEX [3] and SAGE [2] data  $72.5 \pm 5.7$  SNU.

### III. PARAMETERIZATION OF NEUTRINO PRODUCTION RATES

The rate of Be neutrino production as function of the radius is:

$$Q_{\nu_{Be}}(r) = 4\pi r^2 n_e(r) n_7(r) \lambda_{e7}(T(r)) \quad (5a)$$

$$= 4\pi r^2 P_{Be}(r) n_3(r) n_4(r) \lambda_{34}(T(r)), \quad (5b)$$

where  $n_x$  ( $x = 1, 3, 4, 7, e$ ) is the number density of particles (protons,  $^3\text{He}$ ,  $^4\text{He}$ ,  $^7\text{Be}$  nuclei, electrons),  $P_{Be} = \lambda_{e7} n_e / [\lambda_{e7} n_e + \lambda_{17} n_1]$  is the electron capture probability and  $\lambda_{ij} = \langle v \sigma_{ij} \rangle$  is the reaction rate averaged over the Maxwellian distribution of the relative velocities, which is a known function of temperature and does not depend on solar model.

Since the  $^7\text{Be}$  electron-capture-lifetime in the solar core is very short,  $\tau_e(^7\text{Be}) \approx 1$  yr, the equilibrium value  $n_7 = n_3 n_4 \lambda_{34} / (n_e \lambda_{e7} + n_1 \lambda_{17})$  has been substituted into Eq. (5a) to obtain Eq. (5b). With  $P_{Be} \approx 1$ , the rate of Be neutrino production becomes:

$$Q_{\nu_{Be}}(r) = \frac{\pi N_A^2}{3} (1 - X(r)) [r\rho(r)]^2 \lambda_{34}(T(r)) Y_3(r). \quad (5c)$$

After similar transformations, the rate of B neutrino production,

$$Q_{\nu_B}(r) = 4\pi r^2 n_1(r) n_7(r) \lambda_{17}(T(r)) = Q_{\nu_{Be}}(r) \frac{n_1(r) \lambda_{17}(T(r))}{n_e(r) \lambda_{e7}(T(r))}, \quad (6a)$$

becomes

$$Q_{\nu_B}(r) = \frac{\pi N_A^2}{3} \frac{2(1 - X(r))X(r)}{1 + X(r)} [r\rho(r)]^2 \frac{\lambda_{34}(T(r))\lambda_{17}(T(r))}{\lambda_{e7}(T(r))} Y_3(r). \quad (6b)$$

Let us introduce the following scaling variables:

$$x \equiv r/R_{NPZ} \quad (7a)$$

$$\tilde{\rho}(x) \equiv \rho(r)/\rho_{NPZ} \quad (7b)$$

$$y_4(x) \equiv (1 - X(r)) / (1 - X_{NPZ}) \quad (7c)$$

$$y_3(x) \equiv Y_3(r)/Y_{3,NPZ} \quad (7d)$$

$$\Lambda_{34}(x) \equiv \lambda_{34}(T(r))/\lambda_{34}(T_{NPZ}). \quad (7e)$$

The reference radius  $R_{NPZ}$  is taken within the Neutrino Production Zone (NPZ); in practice, we use  $R_{NPZ} = 0.0535R_\odot$ .

The profile function normalizations are  $\tilde{\rho}(1) = y_4(1) = y_3(1) = \Lambda_{34}(1) = 1$ . The total rate of Be neutrino production becomes:

$$Q_{\nu_{Be}} = \frac{\pi N_A^2}{3} R_{NPZ}^3 \rho_{NPZ}^2 (1 - X_{NPZ}) \frac{S_{34}}{S_{34}^{SSM}} \lambda_{34}(T_{NPZ}) Y_{3,NPZ} I_{Be}, \quad (8)$$

where we have defined the dimensionless integral over the profile functions

$$I_{Be} = \int_0^1 dx [x\rho(x)]^2 y_4(x) \Lambda_{34}(x) y_3(x), \quad (9)$$

and  $\lambda_{34}$  is calculated with the SSM temperature profile (the dependence on the cross section has been explicitly taken into account by  $S_{34}$ ).

In practice, we can use  $\rho_{NPZ} = \rho_{NPZ}^{SSM}$  and  $X_{NPZ} = X_{NPZ}^{SSM}$ , and in the integral  $\tilde{\rho}(x) = \tilde{\rho}^{SSM}(x)$  and  $y_4(x) \approx y_4^{SSM}(x)$ , since these quantities are strongly constrained by

helioseismology and the dependence of the results on their precise value is not strong. On the contrary,  $\Lambda_{34}(x)$  and  $y_3(x)$  are not directly constrained by helioseismology and can be different from the SSM: therefore, we shall study the effects of their change. Therefore, the Be neutrino production rate can be expressed as

$$\frac{Q_{\nu_{Be}}}{Q_{\nu_{Be}}^{SSM}} = \frac{S_{34}}{S_{34}^{SSM}} \frac{\lambda_{34}(T_{NPZ})}{\lambda_{34}(T_{NPZ}^{SSM})} \frac{Y_{3,NPZ}}{Y_{3,NPZ}^{SSM}} \frac{I_{Be}}{I_{Be}^{SSM}}. \quad (10a)$$

Notice that  $\lambda_{34}(T)$  is a known function of  $T$ , independent of the solar model.

Similarly, the B neutrino production rate can be expressed as

$$\frac{Q_{\nu_B}}{Q_{\nu_B}^{SSM}} = \frac{S_{34}}{S_{34}^{SSM}} \frac{S_{17}}{S_{17}^{SSM}} \frac{\eta(T_{NPZ})}{\eta(T_{NPZ}^{SSM})} \frac{Y_{3,NPZ}}{Y_{3,NPZ}^{SSM}} \frac{I_B}{I_B^{SSM}} \quad (10b)$$

where

$$\eta(T) \equiv \frac{\lambda_{34}(T)\lambda_{17}(T)}{\lambda_{e\tau}(T)} \quad (11)$$

is another known solar-model-independent function of  $T$ , and

$$I_B = \int_0^\infty dx [x\rho(x)]^2 \frac{y_4(x)(1-y_4(x))}{2-y_4(x)} H(x) y_3(x) \quad (12)$$

where  $H(x)$  is another profile function:

$$\eta(T(r)) \equiv \eta(T_{NPZ})H(x), \quad (13)$$

whose normalization is also  $H(1) = 1$ .

At this point, we should discuss the role of the normalization radius  $R_{NPZ}$ . Equations (10) show that the only dependence on  $R_{NPZ}$  left is in the profile functions  $I$ . As long as we compare models with the same profiles, the functions  $I$  cancel and there remains no dependence on  $R_{NPZ}$ . However, we are interested also in models with non-SSM profiles. In this case variations of the reference radius modify, in principle, the ratios  $I/I^{SSM}$  and consequently the fluxes, when all other parameters stay fixed. The important point is that these changes of fluxes and ratios can be absorbed by appropriate variations of other parameters, in particular of  $T_{NPZ}$  and  $Y_{3,NPZ}$ , and therefore, a reference radius does not appear as another free parameter. In particular, we use such a parameterization of the profile deformation (see below) that a variation of the reference radius is equivalent to an overall multiplicative factor for the quantity whose profile deformation is considered.

It is also clear that the choice of the SSM is not essential: Eqs. (10) are valid for any two solar models that satisfy the helioseismic constraints.

### 1. SSM radial profiles

We start our analysis by assuming that the shapes of all radial profiles, including  $T(r)$  and  $Y_3(r)$ , are those of the SSM. Since the SSM gives a good description of the solar structure

and since we rescale all values at  $R_{NPZ}$ , this very reasonable assumption should already be a good approximation. In this case  $I_{Be} = I_{Be}^{SSM}$  and  $I_B = I_B^{SSM}$  in Eqs. (10). Then one obtains

$$\frac{Q_{\nu_{Be}}}{Q_{\nu_{Be}}^{SSM}} = \frac{S_{34}}{S_{34}^{SSM}} \times \left( \frac{T_{NPZ}}{T_{NPZ}^{SSM}} \right)^{17} \times \frac{Y_{3,NPZ}}{Y_{3,NPZ}^{SSM}} \quad (14a)$$

$$\frac{Q_{\nu_B}}{Q_{\nu_B}^{SSM}} = \frac{S_{34}}{S_{34}^{SSM}} \times \frac{S_{17}}{S_{17}^{SSM}} \times \left( \frac{T_{NPZ}}{T_{NPZ}^{SSM}} \right)^{30} \times \frac{Y_{3,NPZ}}{Y_{3,NPZ}^{SSM}}, \quad (14b)$$

where, for convenience and without loss of generality, the (model-independent) temperature dependence of the two functions  $\lambda_{34}(T)$  and  $\eta(T)$  have been approximated by power-law functions (this approximation is quite good in the region of interest  $T_{NPZ}/T_{NPZ}^{SSM} = 1 \pm 0.05$ ):  $\lambda_{34}(T) \sim T^{17}$  and  $\eta(T) \sim T^{30}$ . We shall use these power-law functions from now on.

At this point we are left with four free parameters  $S_{34}, S_{17}, T_{NPZ}$  and  $Y_{3,NPZ}$ . Eqs. (14) show that changing  $Y_{3,NPZ}$  by an overall factor has the same effect as changing  $S_{34}$ . Since  $\nu_B$  and  $\nu_{Be}$  fluxes are proportional to  $Y_{3,NPZ}$ , increasing  $Y_{3,NPZ}$  results in the simultaneous increase of both fluxes without changing the  $\Phi_{Be}/\Phi_B$  ratio. It does not help to solve SNP, making actually the problem even harder.

In Figure 1 the two thin solid curves on both sides of the curve “temp.” (thick solid curve) bound the allowed region. This region is given by Eqs. (14) when  $S_{17}$  and  $S_{34}$  are varied within the limits of Eqs. (4) and the temperature is arbitrary. In this region the best fit to the experimental data is indicated by the small cross labeled 8 ( $\Phi_{Be} = 2.02 \times 10^9 \text{ cm}^{-2}\text{s}^{-1}$ ,  $\Phi_B = 2.34 \times 10^6 \text{ cm}^{-2}\text{s}^{-1}$ ) and it is obtained with  $S_{34} = 0.38 \text{ keV b}$ ,  $S_{17} = 31 \text{ eV b}$  and  $T_{NPZ}/T_{NPZ}^{SSM} = 0.969$ . Even if we are assuming no CNO flux, its  $\chi^2 = 35$  is still quite large: more than  $5\sigma$  away from the experimentally allowed region. It is easy to understand from Fig. 1 that further lowering the temperature below  $T_{NPZ}/T_{NPZ}^{SSM} = 0.969$  does not help, unless one also allows values of  $S_{17}$  larger than 31 eV b (larger upward shifts).

It is instructive to follow some selected trajectories within the allowed region.

We can start for example from the BBP98 SSM, *i.e.*, the diamond in Figure 1.

When the temperature is lowered and the other parameters are kept constant, the fluxes follow the thick solid line labeled “temp.”<sup>1</sup> The heavy dots labeled 1 and 4 correspond to temperatures scaled by 0.98 and 0.95. From these points 1 and 4 one can change  $S_{34}$  (or equivalently  $Y_{3,SSM}$ ) and reach points 2 and 6, respectively. Then one reaches points 3 and 7 by increasing  $S_{17}$ . Trajectories are shown by dashed lines. Going from point 1 to point 2 corresponds to changing  $S_{34}$  from 0.53 to 0.38 keV b, and going from point 2 to point 3 to changing  $S_{17}$  from 19 to 23 eV b. In fact, this set of parameters is the best solution, if one keeps  $S_{17}$  within the range of Eqs (4) and the temperature within 2% of the SSM value. Its  $\chi^2 = 48$ : it excludes the experimental data at more than  $6\sigma$ . For reference, had we taken  $\Phi_{CNO} = \Phi_{CNO}^{SSM}$ , instead of  $\Phi_{CNO} = 0$ , the  $\chi^2$  would have been 82, which excludes the experimental data at more than  $8\sigma$ .

---

<sup>1</sup>This is not the usual temperature solution, where the other parameters, and in particular the <sup>3</sup>He abundance, also change as function of temperature.

Two other possible trajectories corresponding to the lower temperature ( $T_{NPZ}/T_{NPZ}^{SSM} = 0.95$ ) are the one leading to point 5 ( $\chi^2 = 80$ ), which is reached by increasing  $S_{17}$  from 19 to its maximum value 31 eV b, and the one leading to point 7 ( $\chi^2 = 187$ ), which is reached by decreasing  $S_{34}$  from 0.53 to its minimum value 0.38 keV b ( $4 \rightarrow 6$ ) and then increasing  $S_{17}$  from 19 to 31 eV b. Note, that we described these trajectories only for illustration; numerical calculations used directly the parameterizations of Eqs. (14).

## 2. The modified radial profiles

Now we generalize the above analysis and allow the shape of the radial profiles to be different from that of the SSM. Therefore, we do not assume anymore  $I_{Be,B} = I_{Be,B}^{SSM}$  and obtain:

$$\frac{Q_{\nu Be}/Q_{\nu Be}^{SSM}}{Q_{\nu B}/Q_{\nu B}^{SSM}} = \frac{S_{17}^{SSM}}{S_{17}} \times \left( \frac{T_{NPZ}}{T_{NPZ}^{SSM}} \right)^{-13} \times \frac{I_{Be}/I_{Be}^{SSM}}{I_B/I_B^{SSM}}. \quad (15)$$

In comparison with the previous case the only remaining hope is that the ratios  $I_{Be,B}/I_{Be,B}^{SSM}$ , determined by the radial profiles, could improve the agreement with the experimental data.

In particular, a large deformation of the  ${}^3\text{He}$  profile could, in principle, significantly change the integrals  $I_{Be,B}$  circumventing the problem of the too large ratio of boron to beryllium flux; this approach corresponds to the proposal of Cumming and Haxton [17].

In fact, the only profile functions which can significantly affect the integrals  $I_{Be}$  and  $I_B$  are those of the temperature and the  ${}^3\text{He}$  abundance: the former because of the strong temperature dependence of the rates, the latter because of its being basically unconstrained by helioseismology.

To estimate the dependence of these integrals on the temperature and  ${}^3\text{He}$  profiles we introduce the following parameterization:

$$F_\delta(r/R_{NPZ}) \equiv F_{SSM}(r/R_{NPZ}) \times \left( \frac{r + 0.0535R_\odot}{R_{NPZ} + 0.0535R_\odot} \right)^{\pm\delta}, \quad (16)$$

where  $F$  is either the temperature or the  ${}^3\text{He}$  profile. This parameterization keeps the normalization  $F(1) = 1$  fixed, gives larger deformations for larger  $|\delta|$ 's and reproduces the SSM profile when  $\delta = 0$ . Positive (negative)  $\delta$ 's increase (decrease) the function for  $r > 0.0535R_\odot$  relative to  $r < 0.0535R_\odot$ . Since we want a single parameter function, the scale  $0.0535R_\odot$  is kept fixed:  $\delta$  is sufficient to control the first derivative of the profile at  $R_{NPZ}$ . In other words, this parameterization includes all possible changes of the overall normalization and first derivative of the temperature and  ${}^3\text{He}$  profile. Parameterizing differently the deformation in the NPZ (more parameters and/or different functional forms) must lead to similar conclusions, since the beryllium and boron neutrino production region is sufficiently small, so that higher order derivatives result only in small corrections.

In fact, we have explicitly checked that, if we drastically change this scale from  $0.05R_\odot$  to  $0.025R_\odot$  (changes in the other direction are not relevant to the solution of the solar neutrino problem), this new parameterization reproduces the same results within a few



percent, obviously for different values of  $\delta$ 's (for instance, the case  $\delta = -4$  is reproduced by  $\delta = -2.7$ ). The dotted curve in Fig. 2 shows that the difference between the two parameterizations is small in the region where neutrinos are produced. In this respect, we find instructive, and less dependent on the specific parameterization, to consider the changes of the profile at two representative points  $r = 0.01R_\odot$  and  $r = 0.1R_\odot$  of the inner and outer part of the NPZ instead of  $\delta$  itself.

Notice that changing the reference radius  $R_{NPZ} \rightarrow R'_{NPZ}$  in Eq. (16) only give an overall multiplicative factor that can be absorbed in the scale factors  $T_{NPZ}$  and  $Y_{3,NPZ}$ , confirming that the choice of  $R_{NPZ}$  is irrelevant also in the case of deformed profiles.

*Temperature profile* with  $|\delta| = 0.057$  in Eq. (16) results in a maximal temperature correction of about 5% in the relevant region ( $0.01R_\odot < r < 0.1R_\odot$ ). In Table I we report the dependence of  $I_{Be}$  and  $I_B$  on the change of shape of the temperature profile. It is particularly important the relative change of  $I_{Be}/I_B$ . The ratio  $I_{Be}/I_B$  changes at most of about 15%, relative to the SSM ratio. Changes of this magnitude of the  $\nu_B$  and  $\nu_{Be}$  fluxes are compatible with their theoretical uncertainties (about 10% for the  $\nu_{Be}$  and about 30% for the  $\nu_B$  flux). Therefore, modifying the temperature profile does not help much.

The  ${}^3\text{He}$  profile affects the neutrino fluxes much more strongly, because the  ${}^3\text{He}$  abundance  $Y_3(r)$  is not constrained by helioseismology and is allowed to be considerably different from the SSM shape. One can consider in this case larger values of  $|\delta|$ .

In Table II we report the dependence of  $I_{Be}$  and  $I_B$  on the  ${}^3\text{He}$  profile. Note that increasing the abundance in the center relative to the outer part of the NPZ ( $\delta < 0$ ) has the effect of decreasing the ratio of the Be to B neutrino flux. It is possible to suppress this ratio by a factor almost 0.6 ( $\delta = -4$ ) at the price, however, of increasing (decreasing) the inner (outer) part of the NPZ by a factor about 8 (1/4). Such a change of profile (a factor of thirty over less than  $0.1R_\odot$ ) is really dramatic in comparison with the SSM as one can see in Fig. 2.

In the following we analyse why even large deformation of the  ${}^3\text{He}$  profile can only partially improve the comparison with the experiments. A deformation of the  ${}^3\text{He}$  radial profile that increases the  ${}^3\text{He}$  abundance for  $r < 0.0535R_\odot$  and decreases it for  $r > 0.0535R_\odot$  boosts  $\Phi_B$  relative to  $\Phi_{Be}$ , since the boron neutrinos are produced at smaller radii than beryllium ones. However, such a deformation has the effect of moving both production regions to smaller radii with two consequences: both fluxes increase (even if by different factors) and the difference between the two production regions shrinks. On the one hand, the more we deform the profile the more is difficult to keep boosting  $\Phi_B$  relative to  $\Phi_{Be}$ : this explains why even the large deformation we have considered ( $\delta = -4$  in our parameterization, which corresponds to an increase of  ${}^3\text{He}$  in the inner part of the NPZ relative to the outer part by more than one order of magnitude) can only improve the ratio by a factor 0.64 (see Table II). On the other hand, even if a strong deformation results in the required small  $\nu_{Be}/\nu_B$  ratio, it would be still necessary to strongly reduce both fluxes. This could be achieved either by lowering the temperature or by lowering the overall  ${}^3\text{He}$  abundance (the normalization factor  $Y_{3,NPZ}$ ). The possibility of lowering the temperature is limited by helioseismology, and it does not seem physically possible to strongly reduce the  ${}^3\text{He}$  abundance in the solar core (less strongly towards the center so that the required profile deformation is achieved), since any mixing should *increase* the  ${}^3\text{He}$  in the core.

In Fig. 3 the thick solid line shows the variation of neutrino fluxes with temperature in

the case of the strongest deformation of  ${}^3\text{He}$  profile ( $\delta = -4$ ). The thin solid lines bound the region that is spanned when also  $S_{17}$  and  $S_{34}$  are varied within the limits of Eqs. (4). The best fit point is labeled 4 ( $\Phi_{Be} = 1.72 \times 10^9 \text{ cm}^{-2}\text{s}^{-1}$  and  $\Phi_B = 2.41 \times 10^6 \text{ cm}^{-2}\text{s}^{-1}$ ); it is obtained with  $S_{34} = 0.38 \text{ keV b}$ ,  $S_{17} = 31 \text{ eV b}$  and  $T_{NPZ}/T_{NPZ}^{SSM} = 0.95$  and has a  $\chi^2 = 32$ , or about  $5\sigma$ 's away from the area allowed by experimental data. The trajectory  $2 \rightarrow 3 \rightarrow 4$  shows a possible way to reach the best-fit point 4.

Including contributions of CNO neutrinos to the signals makes the agreement with experimental data even worse.

We could not reach in our calculations the point of Cumming and Haxton (shown in Fig. 1 and Fig. 3 by an asterisk) because of the seismic constraints imposed in our calculations and because we do not allow an overall strong reduction of  ${}^3\text{He}$  in the core, which cannot be caused by mixing.

#### IV. CONCLUSIONS

The solar neutrino experiments have the status of disappearance oscillation experiments. This statement is based on the impossibility of explaining the observed deficit of neutrino fluxes with astrophysical processes not included in SSM's and revised nuclear cross-sections. Helioseismic data strongly constrain the possible non-SSM astrophysical processes.

Recently the idea of  ${}^3\text{He}$  mixing in the solar core has been revived [15,20,21,17]. The abundance of  ${}^3\text{He}$  is not directly constrained by seismic data. In principle this fact opens a road to possible revisions of the SSM predictions for the neutrino fluxes. However, in any realistic model,  ${}^3\text{He}$  mixing is accompanied by other phenomena, *e.g.*, hydrogen is also transported into the core; because of these accompanying phenomena  ${}^3\text{He}$  mixing can be constrained by seismic observations (see [18,11]). We present a more general approach where constraints on the neutrino fluxes are valid for any mechanism of  ${}^3\text{He}$  mixing.

We assume arbitrary  ${}^3\text{He}$  mixing. Some unspecified process brings fresh  ${}^3\text{He}$  from the  ${}^3\text{He}$ -richer outer shells into the solar core where thermal equilibrium is quickly established, but not nuclear equilibrium. Since this process could consist of short mixing episodes, we do not impose the solar-luminosity constraint. The density radial profile is taken from seismic data. Within the accuracy needed for calculations of neutrino fluxes, the  $X(r)$  and  $Y(r)$  profiles are also provided by seismic data. Therefore, the only solar parameters that are needed for model-independent calculations of neutrino fluxes are the temperature  $T$ , the  ${}^3\text{He}$  abundance  $Y_3$ , the astrophysical factors  $S_{34}$  and  $S_{17}$  (cross-sections), and the radial profiles of  $T(r)$  and  $Y_3(r)$ . We allow independent and large variations of  $T$ ,  $S_{34}$  and  $S_{17}$  as given by Eqs. (1) and (4).

Regarding the radial dependence of the temperature,  $T(r)$ , and of the  ${}^3\text{He}$  abundance,  $Y_3(r)$ , we used two approaches.

The first one consists in using the SSM radial dependences. This choice appears reasonable, because B and Be neutrinos are actually produced in a narrow region and distortions of the radial profiles, if not extreme, should not change the fluxes much. Results of this first approach are presented in Fig. 1.

The thick solid line describes the evolution of the fluxes with temperature. The two thin solid lines confine the region allowed by arbitrary variations of  ${}^3\text{He}$  abundance and the

temperature, accompanied by variations of  $S_{34}$  and  $S_{17}$  within the ranges given by Eqs. (4). The cross labeled 8 shows the best fit, which has a very large  $\chi^2 = 35$ .

In the second approach we also allow changes in the shapes of the radial profiles  $T(r)$  and  $Y_3(r)$ . We find that the distortion of the  ${}^3\text{He}$  profile has a much stronger effect on the neutrino fluxes and it is the only important one in our analysis. To improve the agreement with experimental data, the  ${}^3\text{He}$  abundance should, contrary to the SSM case, increase towards the center, as illustrated by the dashed line in Fig. 2. We are aware of no physical mechanism in solar models that could produce such a dependence. We just take an unconventional and very strong radial dependence such as the one shown in Fig. 2 as an *ad hoc* assumption.

With this extremely deformed  ${}^3\text{He}$ -density profile we repeat the exercise of varying the  ${}^3\text{He}$  abundance and temperature in the neutrino production zone, with simultaneous variations of  $S_{34}$  and  $S_{17}$ . In Fig. 3 the allowed region is confined by the two thin solid curves. The best fit to observational data is given by point 4, and it still corresponds to a large  $\chi^2 = 32$ , *i.e.* more than  $5\sigma$  away from the experimentally allowed region.

In all our calculations we have conservatively assumed a vanishing CNO neutrino flux. Inclusion of any amount of CNO neutrinos makes the disagreement with the experimental data worse.

We conclude that practically arbitrary  ${}^3\text{He}$  mixing, which also includes physically unjustified distortions of the  ${}^3\text{He}$  radial profile, and independent variations of temperature and cross-sections cannot explain the observed solar neutrino fluxes.

One might ask, however, whether and to what extent the considered uncertainties, especially in  ${}^3\text{He}$  mixing, can reduce the discrepancy between the SSM solar-neutrino fluxes and observations. The most important source of uncertainty is the  $p + Be$  cross section ( $S_{17}$ ), which affects only the predicted flux of B neutrinos. Taking  $S_{17}$  40% lower than presently used and the core temperature  $T_c$  1.4% lower (as maximally allowed [27] by seismic observations) one arrives at the minimum B-neutrino flux  $3 \cdot 10^6 \text{ cm}^{-2}\text{s}^{-1}$  [28], *i.e.*  $7.4\sigma$  higher than the measured one. It is more difficult to estimate a reasonable effect of  ${}^3\text{He}$  mixing (if this process exists at all). It is constrained by accompanying processes, such as hydrogen mixing, and a realistic model is needed for such calculations. The method used in this work can give only an upper limit of the influence of  ${}^3\text{He}$  mixing on neutrino fluxes. The *ad hoc* assumptions used in this analysis are maximally favorable for this influence, though rather unrealistic.

## REFERENCES

- \* Electronic address: berezinsky@lngs.infn.it  
 † Electronic address: fiorentini@fe.infn.it  
 ‡ Electronic address: marcello.lissia@ca.infn.it
- [1] B. T. Cleveland, *et al.*, in: *Proceedings of the 4th International Solar Neutrino Conf., Max-Planck Institute fuer Kernphysik, Heidelberg, 4–11 April 1997*, edited by W. Hampel, p. 85 (1997);  
 B. T. Cleveland, *et al.*, *Astrophys. J.* **496**, 505 (1998).
- [2] SAGE Collaboration, V. N. Gavrin, *et al.*, in: *Neutrino 98, Proceedings of the XVIII International Conference on Neutrino Physics and Astrophysics, Takayama, Japan, 4–9 June 1998*, edited by Y. Suzuki and Y. Totsuka. To be published in *Nucl. Phys. B (Proc. Suppl.)*.
- [3] T. Kirsten, in: *Neutrino 98, Proceedings of the XVIII International Conference on Neutrino Physics and Astrophysics, Takayama, Japan, 4–9 June 1998*, edited by Y. Suzuki and Y. Totsuka. To be published in *Nucl. Phys. B (Proc. Suppl.)*.
- [4] Y. Suzuki, in: *Proceedings of the 17th International Conference on Neutrino Physics and Astrophysics, Helsinki, Finland, 13–19 June 1996*, edited by K. Enqvist, K. Huitu, and J. Maalami, World Scientific, p. 73 (1997).
- [5] SuperKamiokande Coll., Y. Suzuki, in: *Neutrino 98, Proceedings of the XVIII International Conference on Neutrino Physics and Astrophysics, Takayama, Japan, 4–9 June 1998*, edited by Y. Suzuki and Y. Totsuka. To be published in *Nucl. Phys. B (Proc. Suppl.)*.
- [6] J. Christensen-Dalsgaard, *Nucl. Phys. B (Proc. Suppl.)* **48**, 325 (1996).
- [7] W. A. Dziembowski, *Bull. Astron. Soc. India* **24**, 133 (1996).
- [8] S. Degl’Innocenti, W. A. Dziembowski, G. Fiorentini, and B. Ricci, *Astrop. Physics* **7**, 77 (1997).
- [9] S. Basu *et al.*, *Bull. Astron. Soc. India* **24**, 147 (1996).
- [10] J. N. Bahcall, S. Basu, and M. H. Pinsonneault, *Phys. Lett.* **B 433**, 1 (1998), astro-ph/9805135.
- [11] A. S. Brun, S. Turck-Chieze, and P. Morel, *Ap. J.* **506**, 913 (1998), astro-ph/9806272.
- [12] S. Degl’Innocenti, W. A. Dziembowski, G. Fiorentini, and B. Ricci, *Astrop. Phys.* **7**, 77 (1997);  
 V. Castellani, S. Degl’Innocenti, W. A. Dziembowski, G. Fiorentini and B. Ricci, *Nucl. Phys. B (Proc. Suppl.)* **70**, 301 (1999), astro-ph/9712174;  
 G. Fiorentini and B. Ricci, astro-ph/9905341.
- [13] C. Arpesella *et al.* (LUNA collaboration), *Phys. Lett.* **B 389**, 452 (1996).
- [14] V. Berezinsky, G. Fiorentini, and M. Lissia, *Phys. Lett.* **B 365**, 185 (1996), astro-ph/9509116.
- [15] E. Schatzman, in: *Proceedings of the 4th International Solar Neutrino Conf., Max-Planck Institute fuer Kernphysik, Heidelberg, 4–11 April 1997*, edited by W. Hampel, p. 21 (1997).
- [16] F. W. W. Dilke and D. O. Gough, *Nature* **240**, 262 (1972).
- [17] A. Cumming and W. C. Haxton, *Phys. Rev. Lett.* **77**, 4286 (1996), nucl-th/9608045.

- [18] J. N. Bahcall, M. H. Pinsonneault, S. Basu and J. Christensen-Dalsgaard, Phys. Rev. Lett. **78**, 171 (1997), astro-ph/9610250.
- [19] P. Morel and E. Schatzman, A&A **310**, 982 (1996).
- [20] D. Gough, Annals N. Y. Acad. Sci., **647**, 199 (1992).
- [21] W. C. Haxton, in: *Neutrino 98, Proceedings of the XVIII International Conference on Neutrino Physics and Astrophysics, Takayama, Japan, 4-9 June 1998*, edited by Y. Suzuki and Y. Totsuka. To be published in Nucl. Phys. B (Proc. Suppl.), nucl-th/9810024.
- [22] G. Adelberger, *et al.*, Rev. Mod. Phys. **70**, 1265 (1998), astro-ph/9805121.
- [23] V. Castellani, S. Dgl'Innocenti, G. Fiorentini, M. Lissia and B. Ricci, Phys. Rep. **281**, 309 (1997), astro-ph/9606180.
- [24] A. Dar and G. Shaviv, Ap. J. **468**, 933 (1996), astro-ph/9604009;  
A. Dar and G. Shaviv, Phys. Rep. (1999), astro-ph/9808098.
- [25] N. Hata and P. Langacker, Phys. Rev. **D 52**, 420 (1995), hep-ph/9409372;  
N. Hata and P. Langacker, Phys. Rev. **D 56**, 6107 (1997), hep-ph/9705339;
- [26] J. N. Bahcall and M. H. Pinsonneault, Rev. Mod. Phys. **67**, 781 (1995), hep-ph/9505425.
- [27] B. Ricci, V. Berezinsky, S. Degl'Innocenti, W. A. Dziembowski, and G. Fiorentini, Phys. Lett. **B407**, 155 (1997), astro-ph/9705164.
- [28] V. Berezinsky, Plenary talk at 19th Texas Symposium, 1998, hep-ph/9904259.

## FIGURES

FIG. 1. *Neutrino fluxes allowed by arbitrary  ${}^3\text{He}$  mixing accompanied by independent variations of temperature,  $S_{34}$  and  $S_{17}$  (the  ${}^3\text{He}$  and temperature radial profiles are those of the SSM's).* The horizontal (vertical) axis shows the beryllium (boron) flux; fluxes are measured in units of the reference SSM of Bahcall and Pinsonneault BP95 [26] on the bottom (left) scale, and in  $\text{cm}^{-2}\text{s}^{-1}$  on the top (right) scale. The region allowed by the SSM's (BP95 SSM 90% confidence region) is shown by the dotted ellipse; the diamond shows the BBP98 SSM [10] prediction with the relative  $1\sigma$  errors and the square shows the DS96 [24] SSM. The solid ellipse confines the region allowed at  $3\sigma$  by the experimental data (if there is any contribution to the signals from CNO neutrinos this region becomes smaller). A representative set of nonstandard solar model calculations are shown by small "x" symbols and is taken from the review by Hata and Langacker [25], while the asterisk indicates the  ${}^3\text{He}$  mixing assumption by Cunnig and Haxton [17]. The thick solid curve "temp." gives the evolution of the predictions of the BBP98 [10] model with variations of temperature according to Eqs. (14). In particular points 1 and 4 correspond to temperatures lower than  $T_{SSM}$  by factors 0.98 and 0.95, respectively. When  $S_{17}$  diminishes, points move vertically down; when  $S_{34}$  diminishes, they move diagonally towards the origin. Three trajectories ( $1 \rightarrow 2 \rightarrow 3$ ,  $4 \rightarrow 5$  and  $4 \rightarrow 6 \rightarrow 7$ ) are shown for illustration. The two thin solid curves bound the region allowed by arbitrary changes of the  ${}^3\text{He}$  density and of the temperature, accompanied by variations of  $S_{34}$  and  $S_{17}$  within the limits given by Eqs. (4). The best fit to the experimental data is labeled "8" and has the (too large)  $\chi^2 = 35$ .

FIG. 2. *Profiles of the  ${}^3\text{He}$  abundance normalized to 1 at  $R_{NPZ} = 0.0535R_{\odot}$ .* The solid curve shows the profile in the SSM, while the dashed one shows the profile corresponding to the largest deformation considered in this paper, *i.e.*,  $\delta = -4$  in Eq. (16) and in Table II; the dotted curve is an example of different parameterization as discussed in the text.

FIG. 3. *Same as Fig. 1, but with a modified radial profile of the  ${}^3\text{He}$  abundance.* This case corresponds to the maximal distortion ( $\delta = -4$ ) of the SSM profile considered in this work (see Table II and Fig. 2). The temperature trajectory (towards lower temperatures) is shown by the thick solid curve "temp.". The points 1 and 2 correspond to temperatures lower than  $T_{SSM}$  by factors 0.98 and 0.95, respectively. The trajectory  $2 \rightarrow 3 \rightarrow 4$  is shown for illustration: along the track  $2 \rightarrow 3$   $S_{34}$  decreases by a factor 0.38/0.53, while along the track  $3 \rightarrow 4$   $S_{17}$  increases by a factor 31/19. The two thin solid curves bound the allowed region. For comparison the region allowed when keeping the SSM radial profile (see Fig. 1) is bound by the two dotted lines (thin solid lines in Fig. 1). The best fit is given by point 4 ( $\chi^2 = 32$ ), more than  $5\sigma$  away from the experimentally allowed region.

TABLES

TABLE I. Dependence of the integrals  $I_{Be}$  and  $I_B$ , Eqs. (9) and (12), on the temperature profile, parameterized according to Eq. (16). The temperature profile is deformed keeping  $T(R_{NPZ})$  fixed. The first column shows the parameter  $\delta$  used in Eq. (16). The second and third columns give the corresponding change of the integrals  $I_{Be}$  and  $I_B$ , while the fourth column shows the change of their ratio. The last two columns illustrate the tilting of the profile relative to the SSM by reporting  $T/T^{SSM}$  at  $r = 0.01R_\odot$  and  $r = 0.1R_\odot$ .

$\delta$	$I_{Be}/I_{Be}^{SSM}$	$I_B/I_B^{SSM}$	$(I_{Be}/I_B)/(I_{Be}/I_B)_{SSM}$	$T/T^{SSM}(0.01R_\odot)$	$T/T^{SSM}(0.1R_\odot)$
-0.057	0.95	1.21	0.79	1.03	0.98
-0.044	0.96	1.14	0.84	1.02	0.98
0	1.0	1.0	1.0	1.0	1.0
0.044	1.08	0.94	1.15	0.98	1.02
0.057	1.11	0.94	1.18	0.97	1.02

TABLE II. Dependence of the integrals  $I_{Be}$  and  $I_B$ , Eqs. (9) and (12), on the profile of the  ${}^3\text{He}$  abundance. The information is analogous to the one in Table I.

$\delta$	$I_{Be}/I_{Be}^{SSM}$	$I_B/I_B^{SSM}$	$(I_{Be}/I_B)/(I_{Be}/I_B)_{SSM}$	$y_3/y_3^{SSM}(0.01R_\odot)$	$y_3/y_3^{SSM}(0.1R_\odot)$
-4	1.20	1.87	0.64	8.06	0.24
-3	1.05	1.51	0.70	4.78	0.34
-2	0.98	1.27	0.77	2.84	0.49
-1	0.96	1.10	0.87	1.69	0.70
0	1.0	1.0	1.0	1.0	1.0
1	1.11	0.95	1.17	0.59	1.43
2	1.32	0.93	1.41	0.35	2.06
3	1.66	0.96	1.72	0.21	2.95
4	2.23	1.03	2.16	0.12	4.24

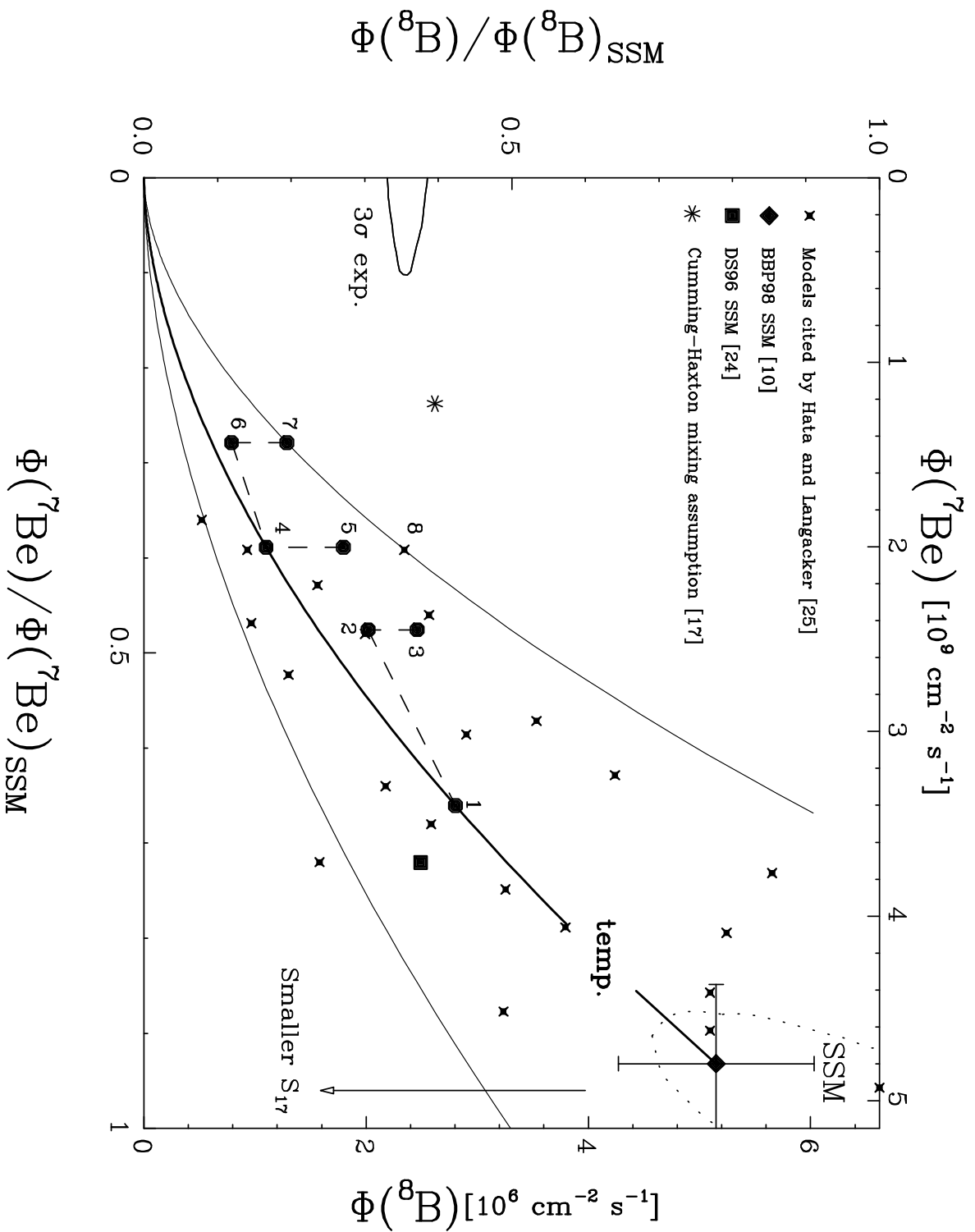


Fig. 1  
Berezinsky et al.: Solar ... He3 mixing



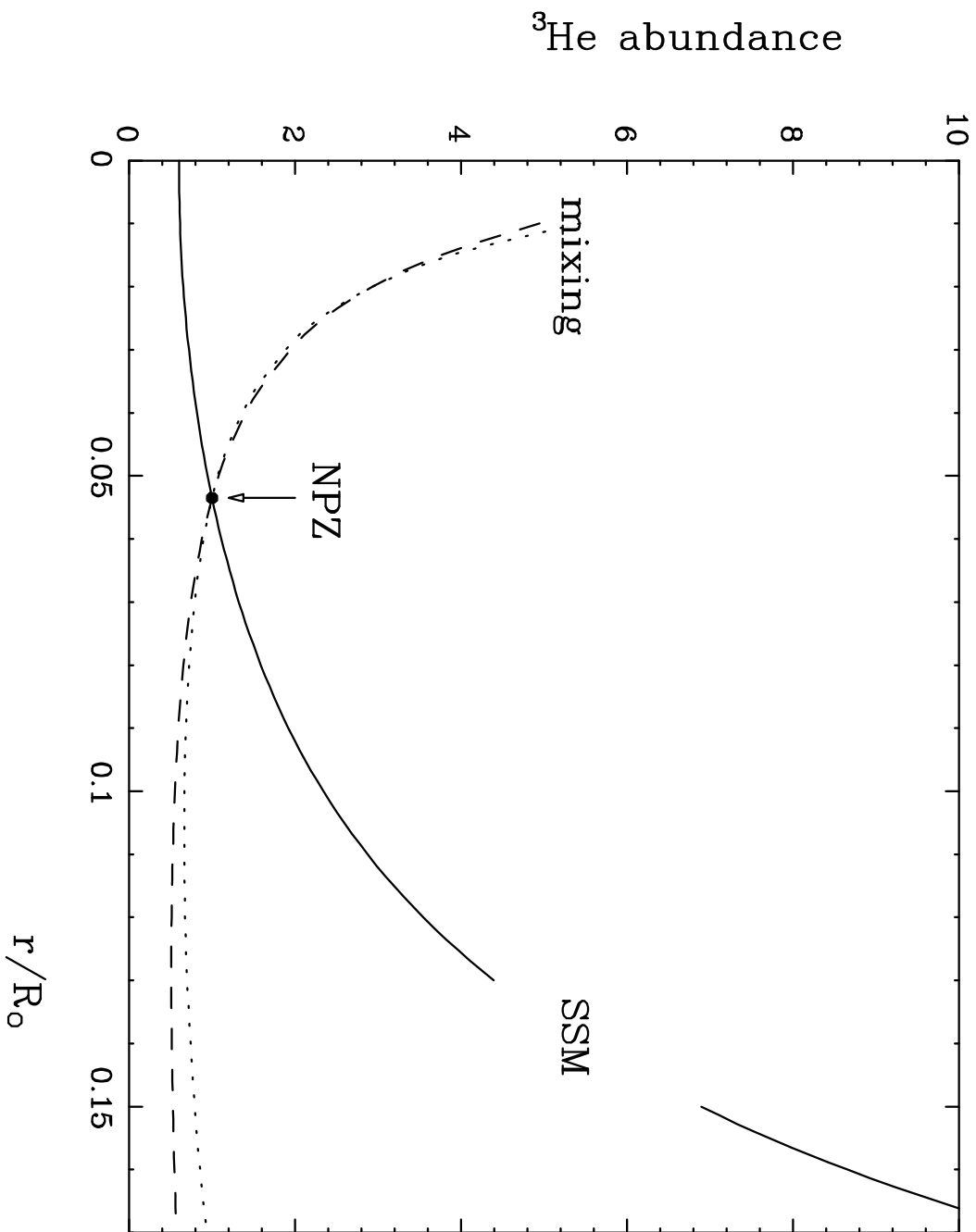


Fig. 2  
Berezinsky et al.: Solar ... He3 mixing

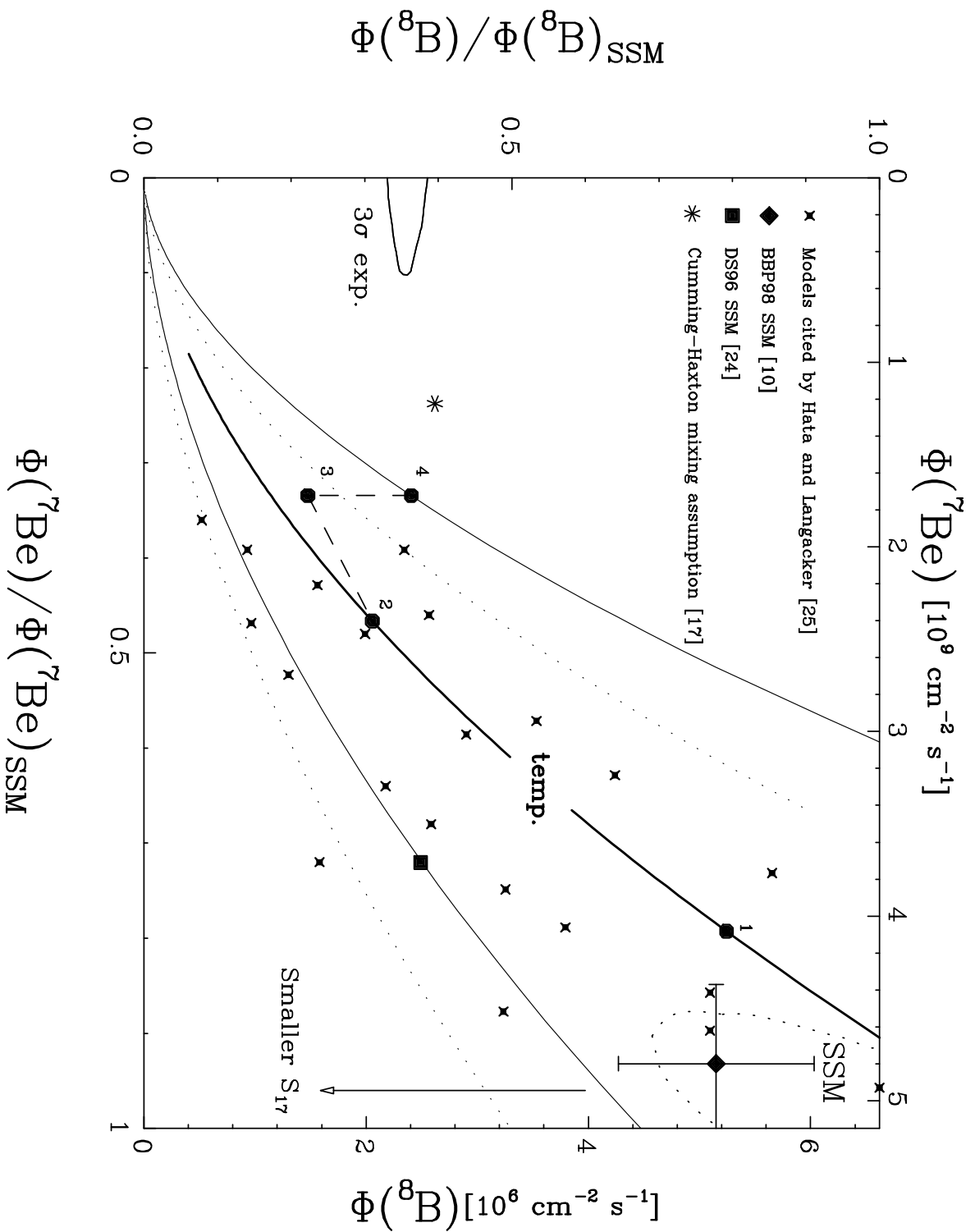


Fig. 3  
Berezinsky et al.: Solar ... He3 mixing